

Particle Resonances in Tokamaks

Roscoe White
Andy Bierwage

Princeton 2020

Resonances of high energy particles in magnetic confinement devices due to electromagnetic instabilities

Outline

Motivation

ORBIT simulations

Resonance

DIII-D

ITER

JT60-U

JT60-U Reversed Shear

Conclusion

Motivation

- Resonances of high energy particles in magnetic confinement devices due to electromagnetic instabilities can strongly modify the distribution.
- The existence of a mode particle resonance depends on properties of the equilibrium, particle trajectories and perturbation mode harmonic content.
- Different methods for finding resonance location and energy dependence are developed.
- We show that if mode resonances exist at low particle energy they very likely also exist at high energy, thus modifying high energy beam particles and fusion products
- Resonance can exist by mode modification of orbit helicity for large mode amplitude

Hamiltonian Guiding Center Code

The equilibrium magnetic field is given by

$$\vec{B} = g\nabla\zeta + I\nabla\theta + \delta\nabla\psi_p, \quad (1)$$

The Hamiltonian is $H = (\rho_{\parallel} - \alpha)^2 B^2 / 2 + \mu B + \Phi$

$$\alpha = \sum_{m,n} A_n \alpha_{m,n}(\psi_p) \sin(\Omega_{mn}), \quad \Phi = \sum_{m,n} A_n \Phi_{m,n}(\psi_p) \sin(\Omega_{mn}),$$

$$\Omega_{mn} = n\zeta - m\theta - \omega_n t - \phi_n,$$

We will be interested in poloidal and toroidal motion

$$\dot{\theta} = \frac{\rho_{\parallel} B^2}{D} (1 - \rho_{\parallel} g') + \frac{g}{D} (\mu + \rho_{\parallel}^2 B) \frac{\partial B}{\partial \psi_p},$$

$$\dot{\zeta} = \frac{\rho_{\parallel} B^2}{D} (q + \rho_{\parallel} I'_{\psi_p}) - \frac{I}{D} (\mu + \rho_{\parallel}^2 B) \frac{\partial B}{\partial \psi_p}.$$

where $D = gq + I + \rho_{\parallel} (gI'_{\psi_p} - Ig'_{\psi_p})$.

Resonance

An unperturbed orbit is periodic in θ and ζ .

For resonance with a mode a particle orbit must periodically return to experience the same perturbation

This requires, since mode is a function of θ and $n\zeta - \omega t$

$$(n\omega_\zeta - \omega)T = 2\pi p, \quad \omega_\theta T = 2\pi l$$

$\omega_\theta, \omega_\zeta$ average poloidal and toroidal frequencies
 ω the mode frequency, n the toroidal mode number
 T some time interval, and p, l integers.

$$p = \frac{(n\omega_\zeta - \omega)l}{\omega_\theta}.$$

This equation must be solved with integers p, l .

Poloidal Elliptic Periodicity

The integer p is the number of poloidal elliptic points of the resonance.

Consider a time interval T such that $nl\omega_\zeta T = 2\pi c$ with c integer

Then we find $\omega_\theta T = 2\pi c/p - \omega l T/p$.

Thus $\theta = \omega_\theta T$ for $c = 0, 1, 2, \dots, p-1$ can take on p values in the interval $[0, 2\pi]$ about $-\omega l T/p$.

The toroidal angle values are $\omega_\zeta T = 2\pi c/nl$, giving nl elliptic points toroidally with $c = 0, 1, 2, \dots, nl-1$.

Values of $l > 1$ correspond to nl toroidal elliptic points instead of n .

Poloidal periodicity is not changed by higher values of l

Because of drift, resonance periodicity in θ is given by one of the poloidal mode harmonics m only at very low energy.

The drifts cause coupling to higher or lower poloidicity.

For high energy particles the poloidal drift motion is primarily $\cos(\theta)$, leading principally to coupling to harmonics with $m \pm 1$.

Orbit Helicity

Most resonances of interest occur in the space of co-passing particles
The particle orbit helicity h is

$$h = \frac{\omega_\zeta}{\omega_\theta}, \quad p = nlh - \frac{l\omega}{\omega_\theta}$$

Both ω_ζ , ω_θ approximately linear in v_\parallel .

At high particle energy where $n\omega_\zeta \gg \omega$, $p = nlh$.

At low particle energy where $n\omega_\zeta \ll \omega$, $p = -\infty$.

Except for drift terms proportional to $\partial B / \partial \psi_p$

which changes sign left or right of the magnetic axis

and terms in g' and I'_{ψ_p} , both small, at low energy $h \simeq q(\psi_p)$.

At higher energy we note that the drift term for θ is larger
and has the opposite sign of that for ζ .

High energy co-moving particles spend more time

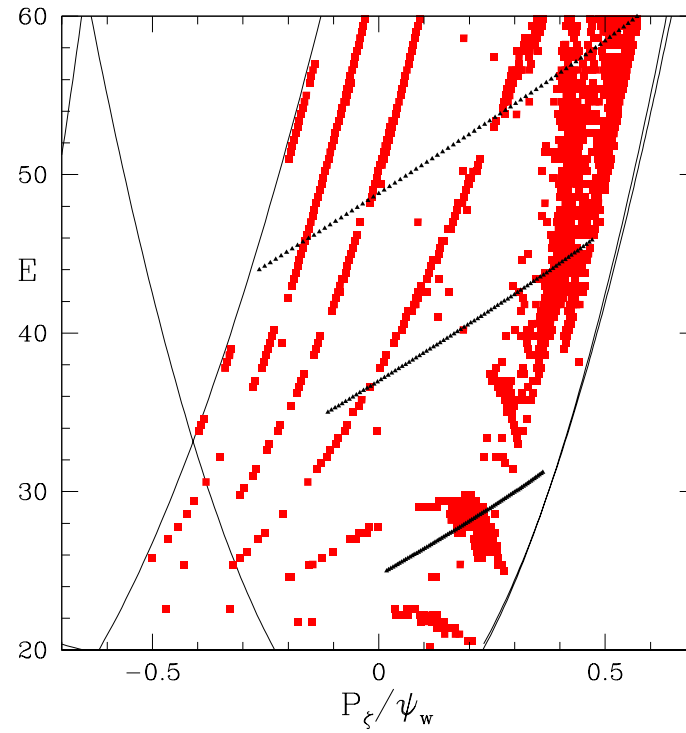
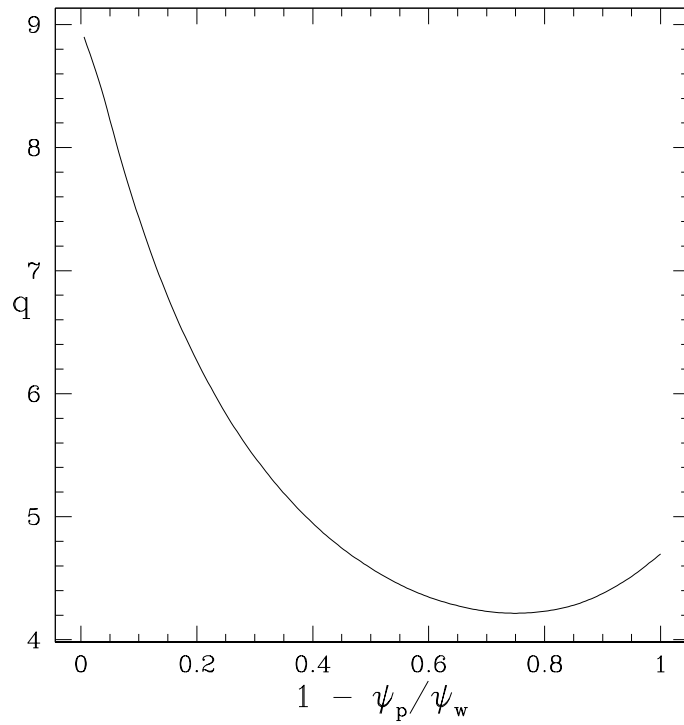
to the right of the axis, where $\partial B / \partial \psi_p < 0$,

so $\dot{\theta}$ decreases and $\dot{\zeta}$ increases with energy, causing h to increase.

The opposite is the case for counter moving ions.

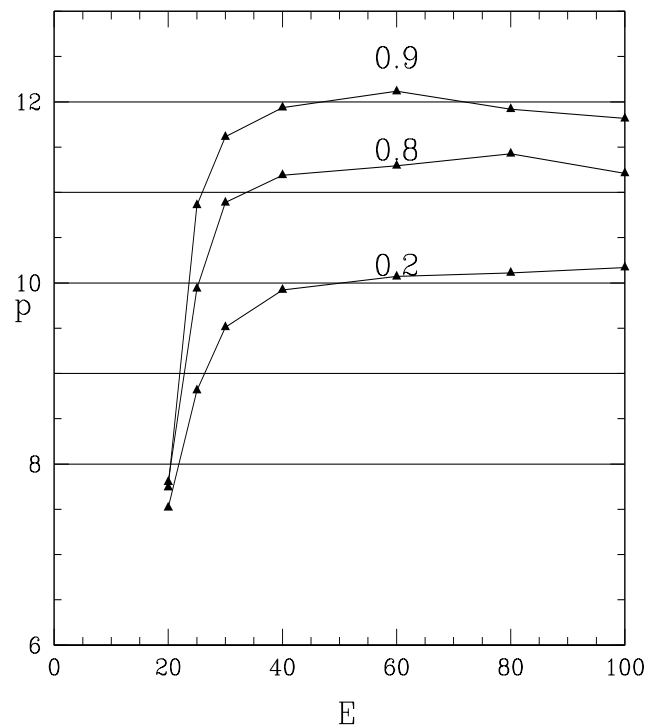
q profile and resonances for the $n = 3$, TAE mode with $10 \leq m \leq 23$, observed in DIII-D in shot 122117.

Broken KAM surfaces determined by phase vector rotation



$$p = nlh - \frac{l\omega}{\omega_\theta}$$

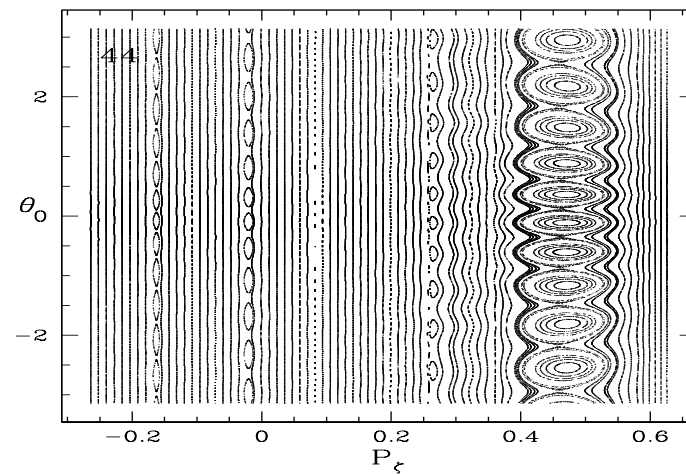
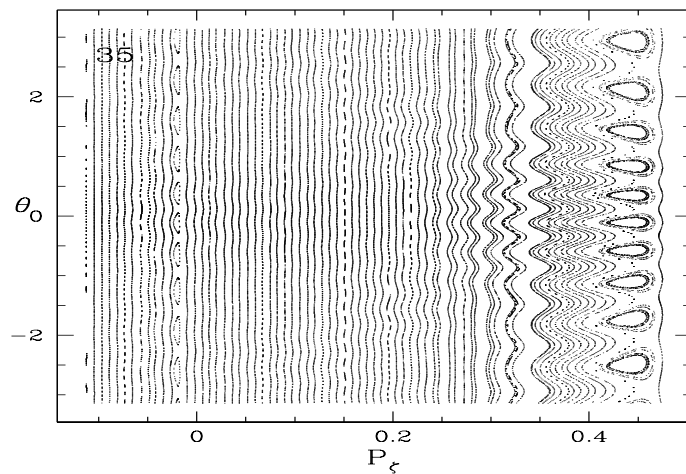
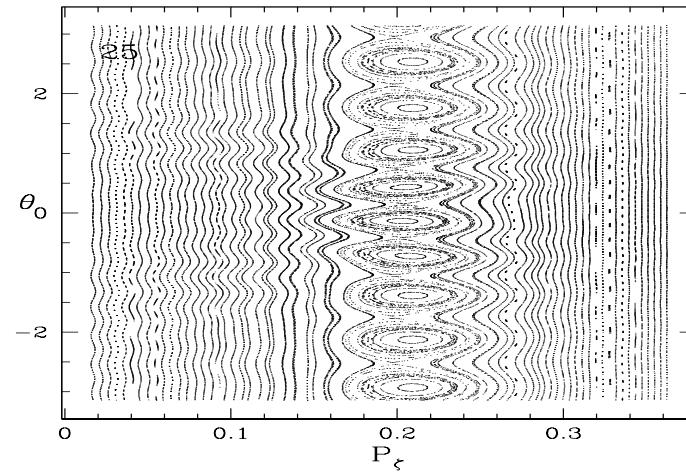
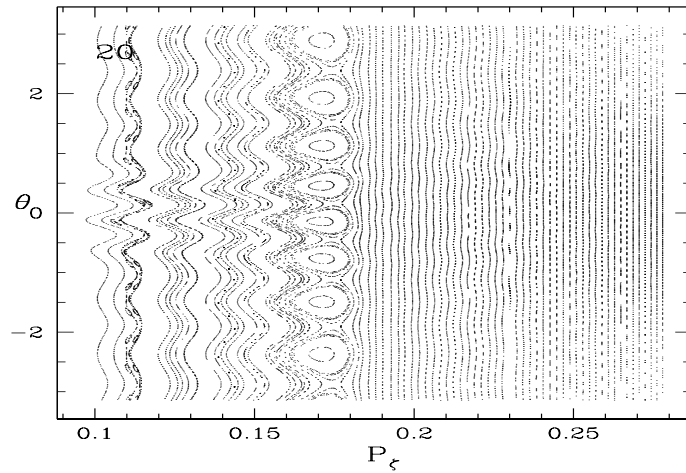
Ellipticity period DIII-D



Ellipticity period $p = (n\omega_\zeta - \omega)/\omega_\theta$ vs energy for three different flux surfaces. $\psi_p/\psi_w = 0.2, 0.8, 0.9$. ω_θ and ω_ζ determined by launching particles. As the particle energy increases, both ω_ζ and ω_θ increase linearly in velocity. The mode transitions from one resonance to another. Asymptotic values are reached over the whole plasma by $E = 40$ keV. Values of $p = 8, 9$ are only possible at energies below 30 keV

Poincare

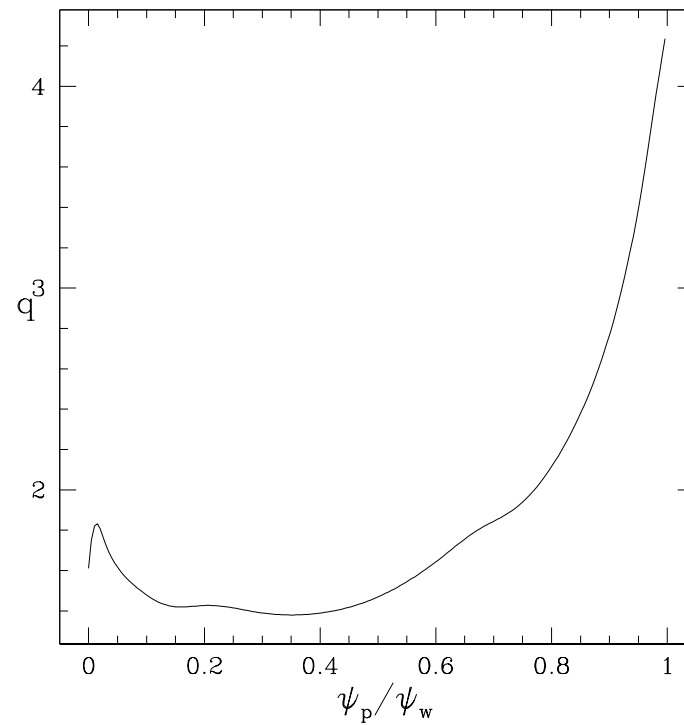
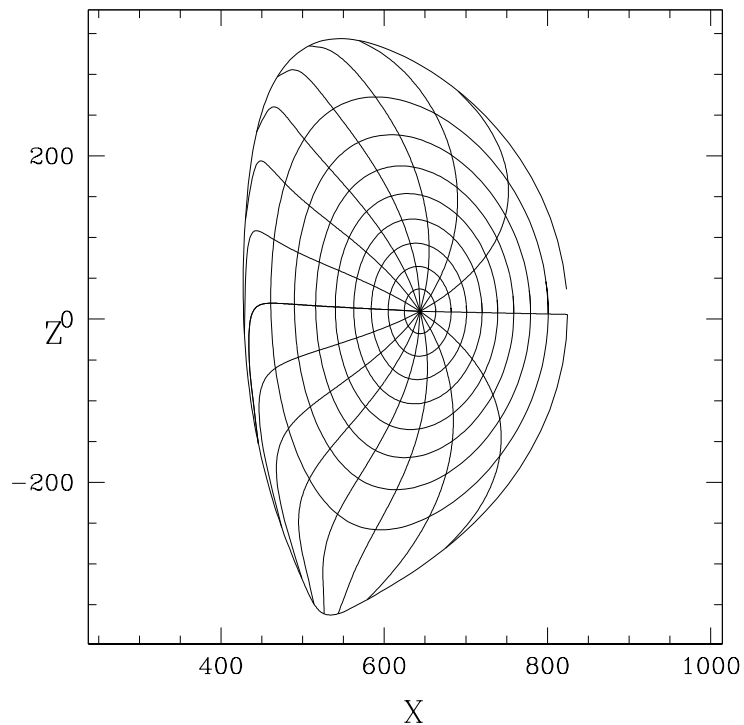
Poincaré plots showing resonances at $E = 21$ ($p = 8$), $E = 25$ ($p = 9$), $E = 35$ ($p = 10,10$), and $E = 44$ ($p = 12,11,10,10$) keV



ITER

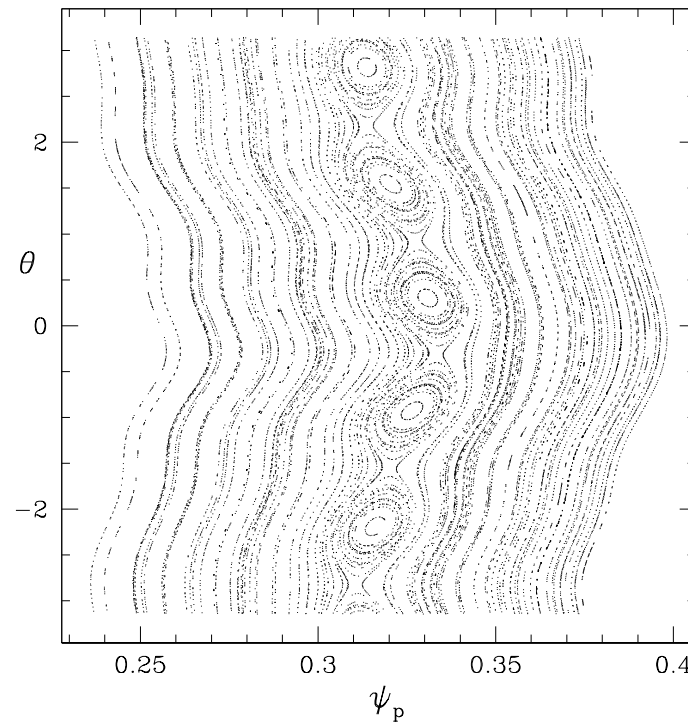
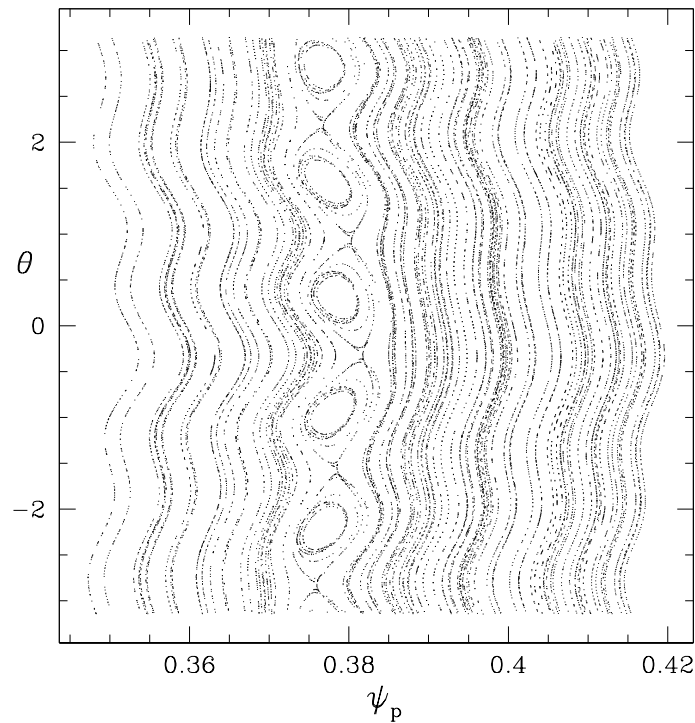
ITER equilibrium and q profile.

Low frequency modes used to try to remove Helium ash,
but energy saturation of p give also resonances at high energy,
causing loss of high energy alpha particle as well as ash.



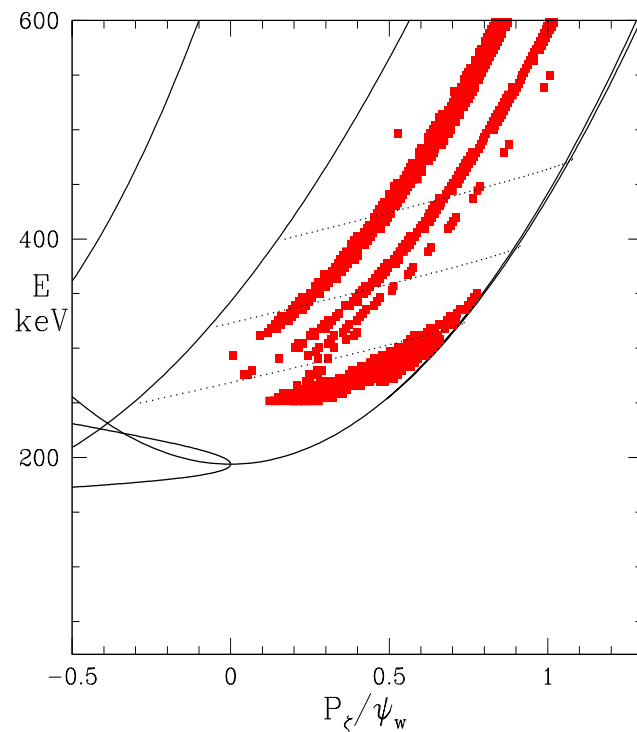
Poincare plots for ITER resonance

Poincaré plots, 6 kHz $m/n = 6/4$ mode. ITER 20 keV and 1 MeV
Aside from the increased particle drift, the resonance is practically unchanged even at this high energy. $p = 5$



JT60-U.

High value of μ , $\mu B = 194$ keV.



Determination of resonances JT60-U
50 kHz 2/1 mode showing two strong
bands of resonances in the center
extending to high energy

There is also a resonance that exists only
below 350 keV, deep in the plasma.

As the energy is increased,
this resonance moves inward
until at 350 keV it passes through
the magnetic axis and thus disappears.

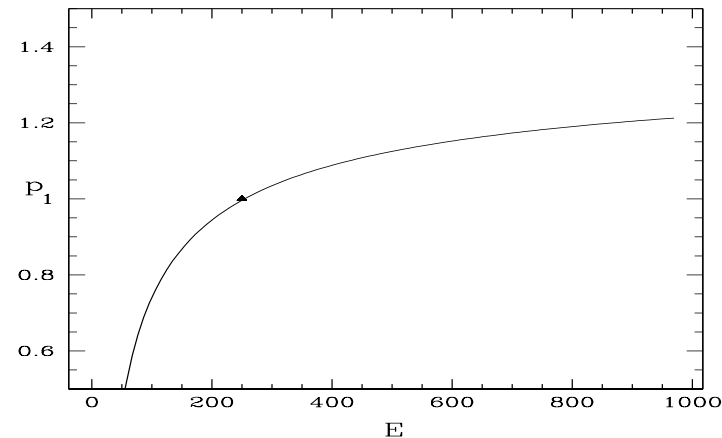
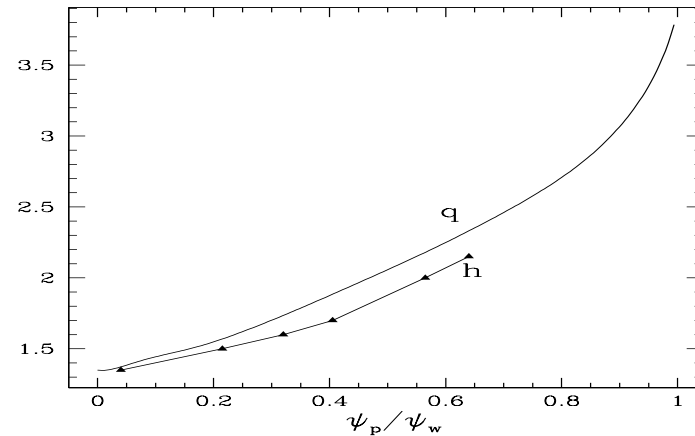
JT60-U Lowest energy Resonance

Lowest energy resonance
moving to magnetic axis
As the energy increases the
value of p increases, but does
not reach an integer above 1.

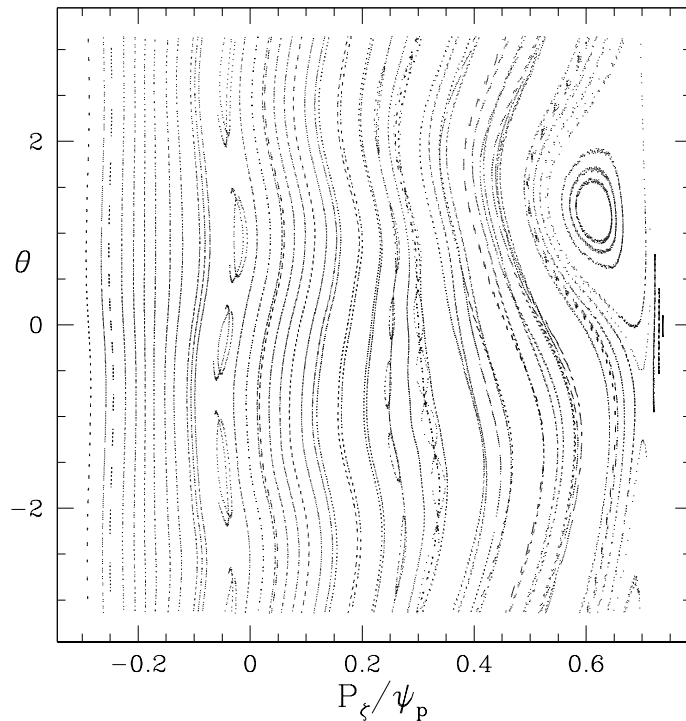
$$p = nh - \frac{\omega}{\omega_\theta}$$

As energy increases the second
term becomes smaller

There are no lower values of q
so the resonance is driven into
the axis and vanishes



JT60-U Poincare plots, bottom



Plots at lower value
of $nE - \omega P_\zeta$.

- Bottom- $p = 4$ resonance
at $P_\zeta = -.05$,
Strong $p = 1$ resonance near
axis.

At all energies the value
of ω_ζ for the two extended
bands is larger than the
mode frequency by at least
a factor of 20, so they are
at asymptotic energies
regarding the value of p .
The number of poloidal el-
liptic points is 3 at $q = 2.5$
and 4 at $q = 2$.

JT60-U High Energy Resonances

Determination of p in the two resonances going to high energy

$$p = \frac{(n\omega_{\zeta} - \omega)l}{\omega_{\theta}}.$$

Plots of $\theta(t)$, $\zeta(t)$

in a resonance band.

ω_{θ} and ω_{ζ} determined.

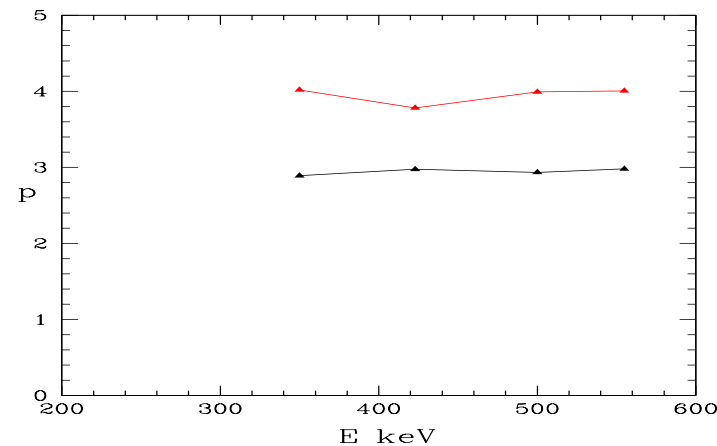
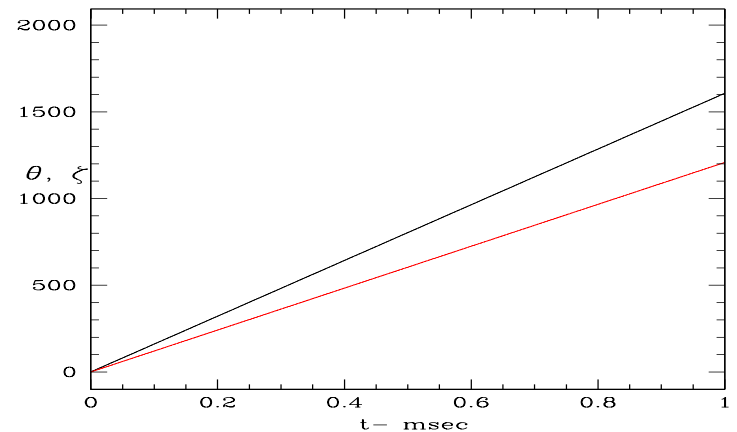
$p \simeq 4$ left band,

$p \simeq 3$ right band.

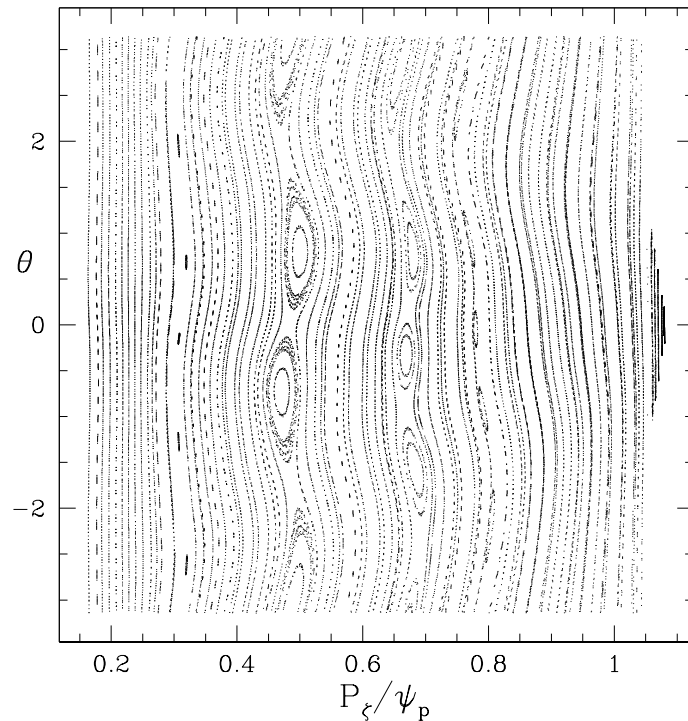
high energy asymptotic regime

Left band $l = 2$ $p = 3$,

Right band $l = 3$, $p = 4$



JT60-U Poincare plots



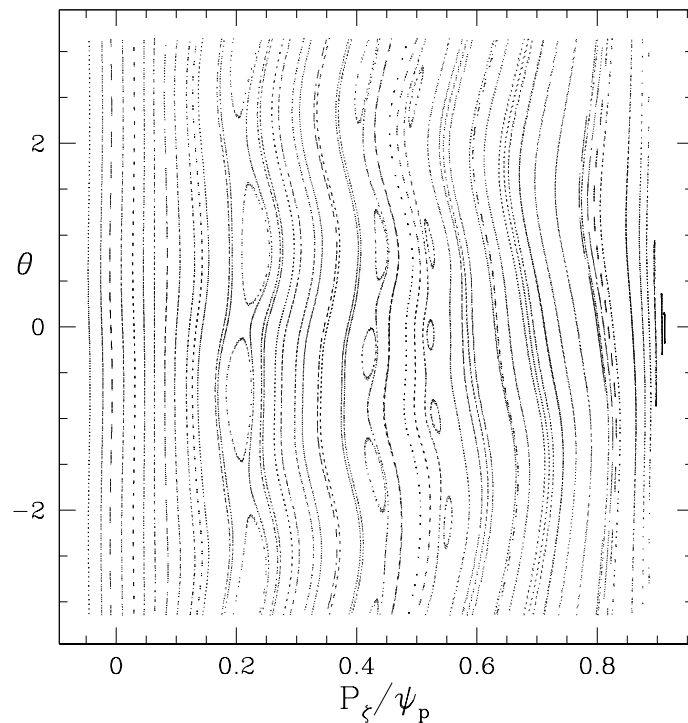
Plots at upper value of $nE - \omega P_\zeta$.

- Two strong resonances as well as a weaker five period resonance at $P_\zeta = 0.3$.

In the left resonance $q \simeq 2.5$, $l = 2$, $p = 3$.

In the right resonance $q \simeq 2.0$, $l = 3$, $p = 4$.

JT60-U Poincare plots, Middle



Plot at middle value of $nE - \omega P_\zeta$.

- Middle- left resonance band with three elliptic points at $P_\zeta = 0.2$
two weaker resonances
four elliptic points $P_\zeta = 0.4$
five at $P_\zeta = 0.55$.

Examine reversed shear profile to see the effect of q near axis

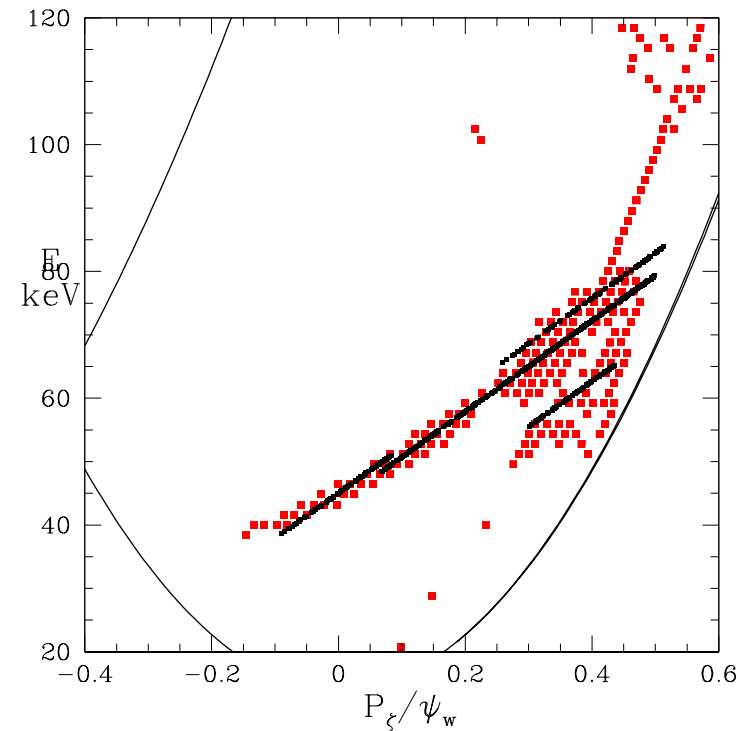
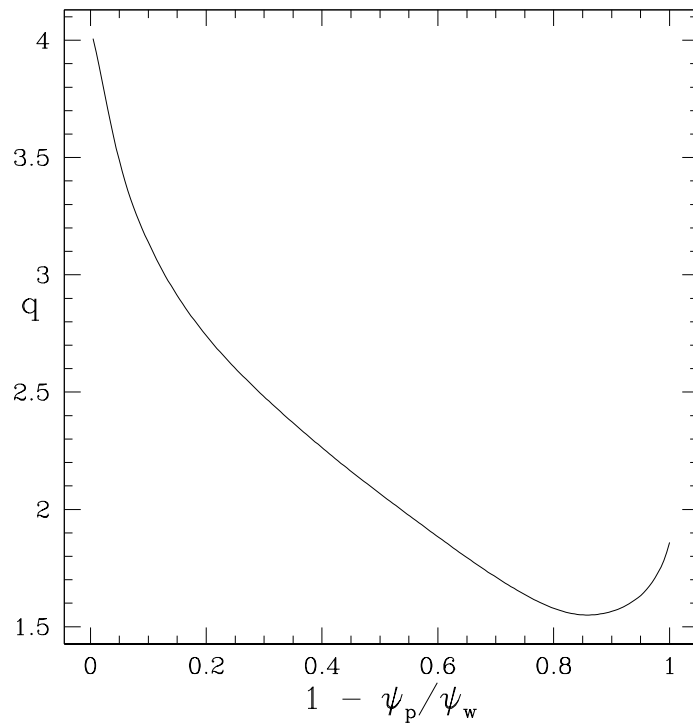
Much lower μ with $\mu B = 14$ keV.

Resonances depend on ω_θ , ω_ζ , not energy.

$\mu B = 194$ keV, resonance 250 keV, $\mu B = 14$ keV, resonance 40 keV

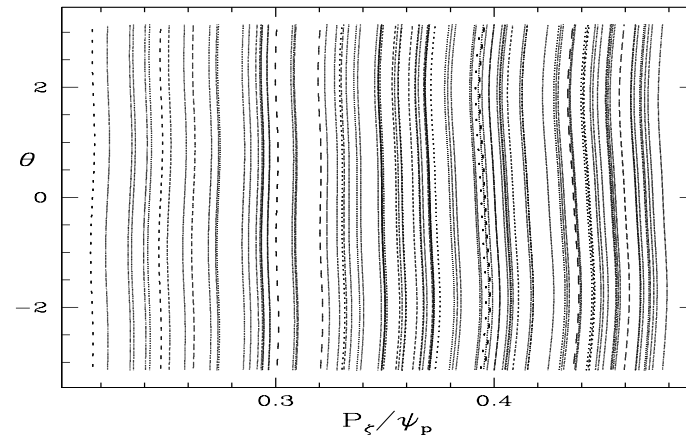
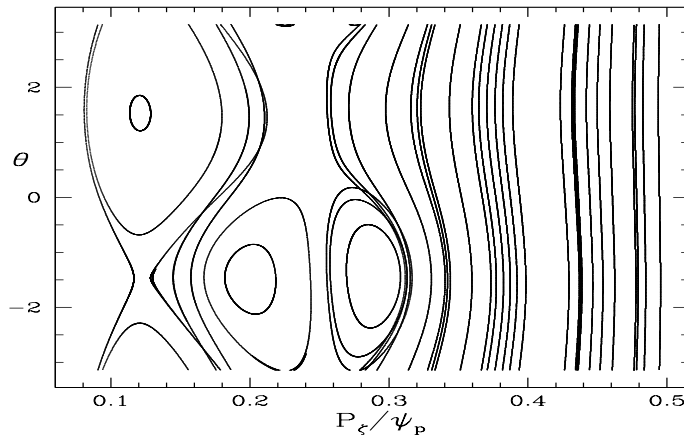
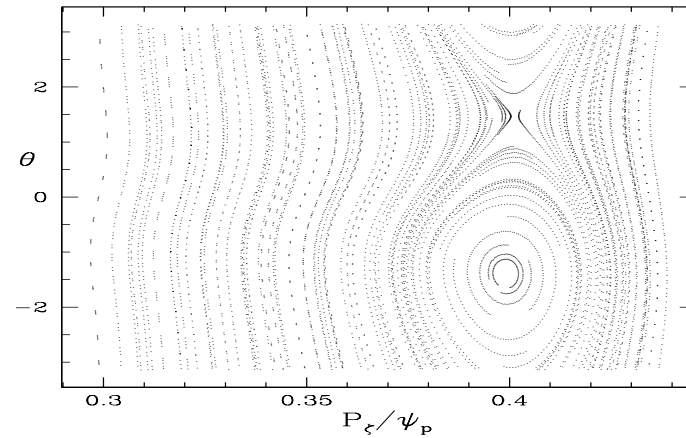
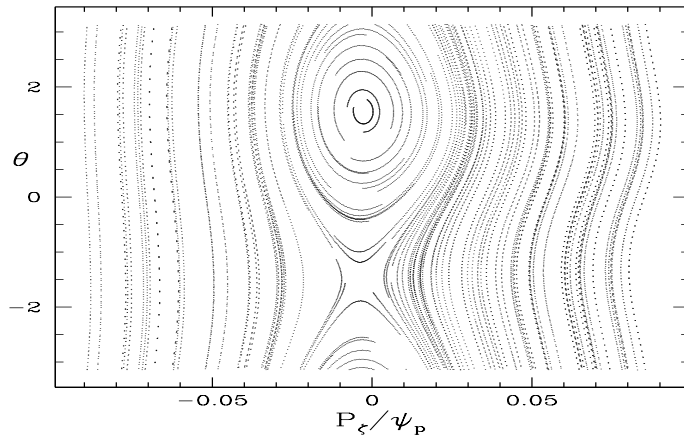
But they are very similar in shape except near axis

Resonance moves toward the axis and is met by a resonance coming out



Poincare for JT60 Reversed Shear

Top left, the $p = 1$ resonance, shown at $E = 45$, $P_\zeta/\psi_w = 0$,
Top right, the $p = 1$ resonance, shown at $E = 60.5$, $P_\zeta/\psi_w = .37$.
Bottom left, Merging of the two resonances at $E = 65$, $P_\zeta/\psi_w = .3$.
Bottom right, no resonance at $E = 75$, $P_\zeta/\psi_w = .35$, $A = 10^{-5}$



Resonances produced by mode modulation of orbital helicity

Plots of h and p for points of the initial low energy mode.

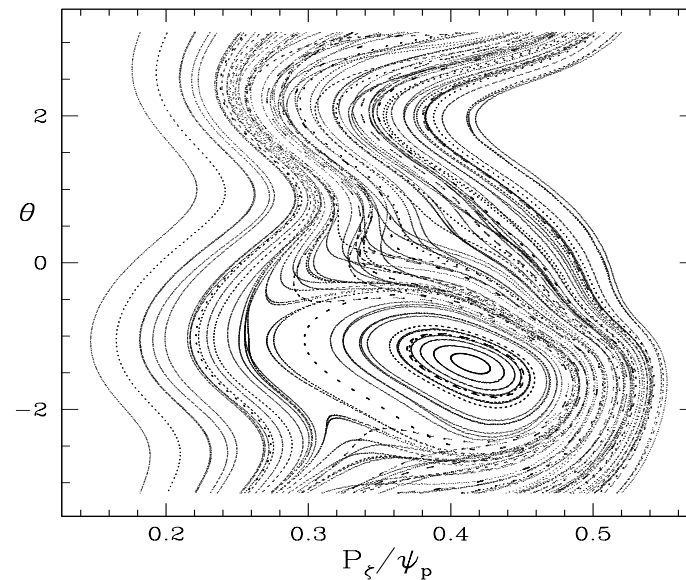
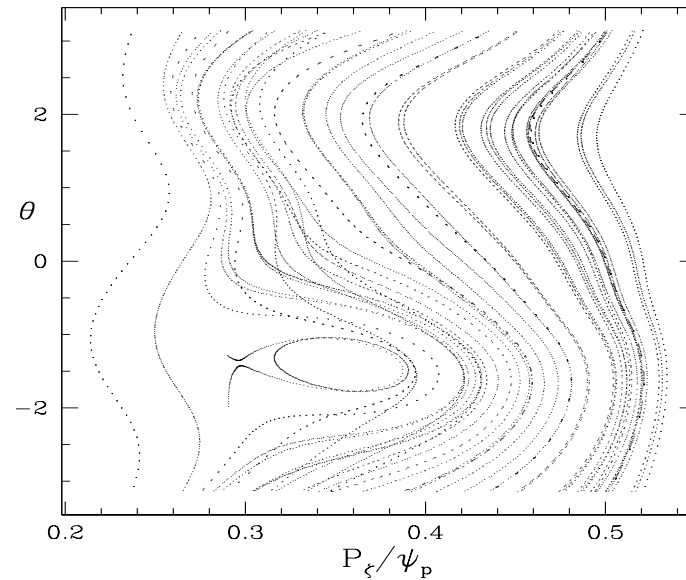
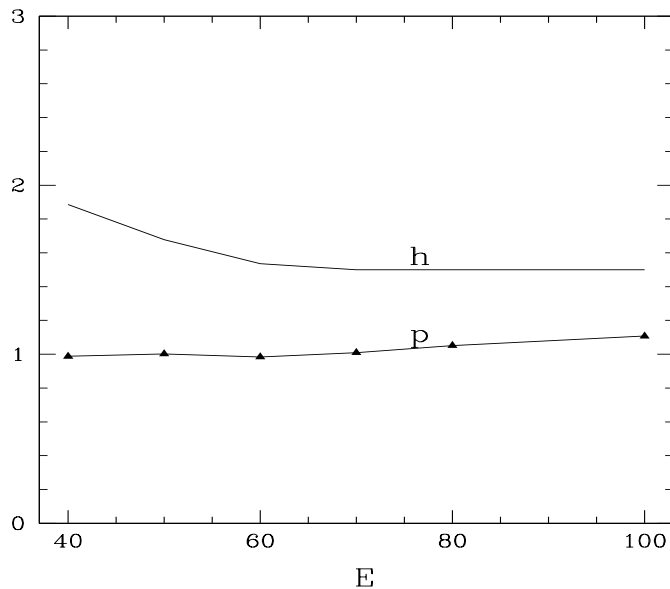
We see $p = 1$,

from 40 to 73 keV.

$p > 1$ for $E > 73$ keV

mode modulation resonance produced at $E = 75$,

$A = 2 \times 10^{-4}$, $A = 5 \times 10^{-4}$



Conclusion

High energy particle resonances are important concerning the existence of a dense fusion capable particle distribution.

They can modify the distribution and even induce particle loss.

Analytic expression found for p , elliptic points of a resonance.

Energy dependence, with poloidal helicity p vs E given.

Depend on parallel velocity, not energy, so μ not important.

Resonances in DIII-D, ITER, and JT60-U are examined.

Resonances existing at low particle energy are very likely to persist at higher energy.

Examples of resonance existing only at low energy are found

Resonance can exist by mode modulation of orbital helicity when p is close to integer.